



## Conceptual design and initial evaluation of a neutron flux gradient detector

Downloaded from: <https://research.chalmers.se>, 2022-11-19 13:27 UTC

Citation for the original published paper (version of record):

al-Dbissi, M., Vinai, P., Borella, A. et al (2022). Conceptual design and initial evaluation of a neutron flux gradient detector. Nuclear Instruments and Methods in Physics Research, Section A: Accelerators, Spectrometers, Detectors and Associated Equipment, 1026.  
<http://dx.doi.org/10.1016/j.nima.2021.166030>

N.B. When citing this work, cite the original published paper.



# Conceptual design and initial evaluation of a neutron flux gradient detector

Moad Aldbissi<sup>a,b,\*</sup>, Paolo Vinai<sup>a</sup>, Alessandro Borella<sup>b</sup>, Riccardo Rossa<sup>b</sup>, Imre Pázsit<sup>a</sup>

<sup>a</sup> Division of Subatomic, High Energy and Plasma Physics, Chalmers University of Technology, 412 96 Göteborg, Sweden

<sup>b</sup> Belgian Nuclear Research Centre, SCK CEN, 2400 Mol, Belgium

## ARTICLE INFO

### Keywords:

Neutron flux gradient detector  
Scintillation detector  
Light guiding fiber  
Monte Carlo

## ABSTRACT

Identification of the position of a localized neutron source, or that of local inhomogeneities in a multiplying or scattering medium (such as the presence of small, strong absorbers) is possible by measurement of the neutron flux in several spatial points, and applying an unfolding procedure. It was suggested earlier, and it was confirmed by both simulations and pilot measurements, that if, in addition to the usually measured scalar (angularly integrated) flux, the neutron current vector or its diffusion approximation (the flux gradient vector) is also considered, the efficiency and accuracy of the unfolding procedure is significantly enhanced. Therefore, in support of a recently started project, whose goal is to detect missing (replaced) fuel pins in a spent fuel assembly by non-intrusive methods, this idea is followed up. The development and use of a dedicated neutron detector for within-assembly measurements of the neutron scalar flux and its gradient are planned. The detector design is based on four small, fiber-mounted scintillation detector tips, arranged in a rectangular pattern. Such a detector is capable of measuring the two Cartesian components of the flux gradient vector in the horizontal plane. This paper presents an initial evaluation of the detector design, through Monte Carlo simulations in a hypothetical scenario.

## 1. Introduction

In nuclear engineering, many applications are related to the task of locating the position of a neutron source, or some strong inhomogeneity (e.g. the presence of a strong absorber), from the measurement of the neutron flux in a multiplying or neutron scattering medium. Based on the knowledge of the surrounding material and hence its effect on neutron transport and multiplication, the task can be achieved by an unfolding procedure, i.e. a kind of triangulation process [1,2]. The unfolding relies on the fact that the neutron distribution in the medium can be calculated for any arbitrary position of a hypothetical unknown source or inhomogeneity, and one seeks the position which yields the minimum deviation between the measured and calculated values.

It was suggested earlier that in such inverse tasks of localization, the efficiency and the accuracy of the localization can be improved if, in addition to the usually measured scalar (angularly integrated) neutron flux, the neutron current vector or the gradient of the neutron flux is measured [3]. Both the current and the gradient are vectors, hence they contain more (and independent) information compared to the scalar flux. The feasibility of using the flux gradient in both static and dynamic localization problems in nuclear reactor cores (e.g., finding the position of a static neutron source, the tip of a partially inserted control rod, a vibrating fuel pin, or a vibrating control rod) was demonstrated via calculations [3,4]. Later the possibility of locating the position of a

neutron source in a water tank from the measurement of the scalar flux and its gradient in one single point was demonstrated experimentally, with the unfolding procedure being supported by Monte Carlo simulations [5]. Another work demonstrated experimentally the possibility of using a single detector (whose half circumference was covered by cadmium) to measure the scalar flux and an approximation of the partial currents, and to identify the position of a neutron source in a water tank from such measured quantities [6,7].

The measurement of the flux gradient or the neutron current was made possible by the use of very thin detectors (about 1 mm), developed in Japan [8,9], which allows to obtain the scalar neutron flux with a high spatial resolution. In these detectors a small volume of a mixture of neutron converter and scintillation material is mounted on the tip of a light guiding fiber. In the pilot measurements, only one single fiber was used for the measurement of the flux gradient. The gradient was determined by placing the same detector sequentially in several positions around the circumference of a small circle, and estimating the line integral from the measurements around the circle.

Such an experiment is suitable for a proof-of-concept, but the method is not useful in practical situations. For a fast and reliable measurement of the flux gradient, a dedicated detector can be constructed with several small neutron sensitive volumes, so that the scalar flux is taken in several positions concurrently. The need for such

\* Corresponding author at: Division of Subatomic, High Energy and Plasma Physics, Chalmers University of Technology, 412 96 Göteborg, Sweden.

E-mail addresses: [moad.al-dbissi@chalmers.se](mailto:moad.al-dbissi@chalmers.se) (M. Aldbissi), [vinai@chalmers.se](mailto:vinai@chalmers.se) (P. Vinai), [alessandro.borella@sckcen.be](mailto:alessandro.borella@sckcen.be) (A. Borella), [riccardo.rossa@sckcen.be](mailto:riccardo.rossa@sckcen.be) (R. Rossa), [imre@chalmers.se](mailto:imre@chalmers.se) (I. Pázsit).

<https://doi.org/10.1016/j.nima.2021.166030>

Received 16 November 2021; Accepted 16 November 2021

Available online 17 December 2021

0168-9002/© 2021 The Authors. Published by Elsevier B.V. This is an open access article under the CC BY license

(<http://creativecommons.org/licenses/by/4.0/>).

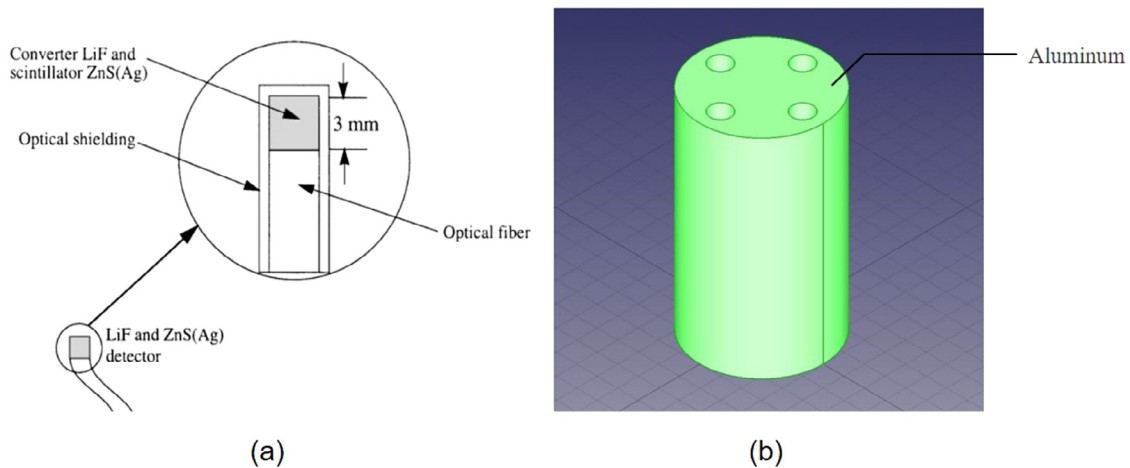


Fig. 1. A scheme of the planned gradient detector (a) The optical fibers with the scintillation material at their tips (b) Aluminum cylinder that acts as a holder for the detectors.

a detector arose recently in connection with a collaboration project between Chalmers and the Belgian Nuclear Research Centre SCK CEN. The goal of the project is to detect and identify, with the help of neutron measurements inside a fuel assembly, whether one or more fuel pins have been removed and replaced by dummy rods, and if so, in which positions. This diversion scenario is known in the safeguards community as detection of partial defects in a fuel assembly [10,11]. The idea is to perform measurements concurrently in several radial points of a fuel assembly, and comparing the measured flux shape with the one calculated from the declared data of the (intact) fuel assembly (to discover the absence of fuel pins), as well as with calculations with defect fuel (to identify the position of the missing pins).

This is clearly an inverse problem, similar to the identification of a neutron source or a strong absorber in a homogeneous medium, although substantially more complicated. First, it is neither the presence of a neutron source, nor that of a strong absorber which has to be identified, rather the absence of a fuel rod, which is, at the same time, a spontaneous neutron emitter (by the decay products), a neutron multiplier (through fission) and a neutron absorber. Second, it is not the single position of one object that has to be identified, rather the positions of an unknown number of missing objects. This problem is thus much more multidimensional than the simple case of identification of one single position.

Some currently existing methods such as the Partial Defect Tester (PDET) are capable of measuring the neutron flux inside a fuel assembly efficiently [10,12]. However, due to the complexity of the unfolding task, it is obvious that measuring not only the scalar flux but also the two components of the flux gradient in a horizontal plane would improve the chances of the identification of the partial defects.

Technically, thin fiber neutron scintillators can be inserted in between the fuel pins, hence a cluster of such detectors can be used to measure the scalar flux simultaneously at several radial positions in an assembly. Since the gradient detector will consist of a cluster of the thin scintillators, it will eventually have larger radial dimensions than the individual fibers. Hence, it can only be inserted into a few special positions within an assembly, such as the detector guide tubes, or possibly some empty control rod channels. It is thought that a combination of a cluster of thin fiber detectors, measuring the scalar flux, and one gradient detector (or possibly a few of them) will provide the most effective solution.

This paper concerns only the investigation of the conceptual design of such a flux gradient detector, suitable for the planned measurements within the fuel assembly, as one phase of the full project. The development of the detector itself will go in several steps. First, a detector design is proposed, consisting of four fiber-mounted scintillation detectors arranged in a rectangular pattern within a cylindrical

holder, and its performance is investigated via numerical simulations. This is the subject of the present paper. The next stage will be the construction of the detector. Experience with using single fibers for flux measurements is available from previous experimental work, hence the necessary technology for constructing the proposed detector is available and accessible. Next, the performance of the detector will be investigated first in pilot measurements, and finally within fresh or spent fuel assemblies, preferably inside the fuel pool.

In the subsequent Sections, first the design of the detector will be described. Then a Monte Carlo model of the detector and a test case is introduced in order to assess the performance of the detector. Finally, the results of the numerical investigation of the performance of the detector are discussed and conclusions are drawn.

## 2. The detector design

Although the diameter of the fiber detectors can be as small as about one mm, the diameter of the gradient detector, allowing the measurement of the flux in different positions from which a reliable estimation of the gradient can be obtained, will be inevitably larger. By aiming at performing measurements within a nuclear fuel assembly, one can use the instrumentation guide tubes of the assembly, which are about 1 cm in diameter. For this study we assumed that a fuel pin is either intact, fully removed or replaced with a stainless steel dummy pin. In this case, only the radial position of the missing pin is interesting in the horizontal plan, and hence the problem is two-dimensional.

A gradient detector, capable of measuring the  $x$  and  $y$  components of the flux gradient (which, in a 2-D cylindrical geometry can also be referred to as the  $r$  and  $\varphi$  components), with the mentioned size limitation, is proposed as follows. Four axial holes in an aluminum cylinder of a diameter of 1 cm serve as holders of four fiber-mounted scintillation detectors, arranged in a rectangular pattern, as shown in Fig. 1. The fibers are inserted into the guide tubes from above, and their tip is covered in the neutron sensitive converter and scintillation material, as shown in Fig. 2. The detector, together with the fibers, is inserted into the instrumentation guide tube and moved to a suitable position sufficiently below the top of the assembly such that the axial flux gradient can be negligible. The two detector pairs at diagonally opposite positions, perpendicular to each other, can be used to measure the two horizontal components of the flux gradient. Aluminum is chosen as the matrix, holding the detectors, due to its easy manufacturing properties, and low neutron absorption cross section.

One remark on the terminology is in order here. The collection of the four fiber-mounted scintillation detectors together constitutes the “gradient detector”. In order to avoid confusion to call both the collection of the four scintillators, as well as the individual scintillators

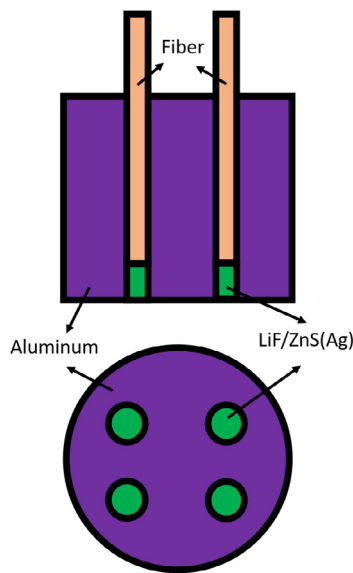


Fig. 2. A vertical and horizontal cross section view of the detector concept.

a “detector”, we will follow the terminology that the four scintillators together, i.e. the gradient detector, will be called the “detector”. Whenever we want to refer to a single fiber-mounted scintillator, it will be simply referred to as a “scintillator”.

### 3. Monte Carlo model of the detector and of a test case

Whereas it is intuitively clear that, in principle, such a detector is suitable to determine the flux gradient, it is useful to assess its performance by detailed simulations. The motivations for this are twofold. First, similar to the case of the ordinary neutron detectors, the presence of the detector, and in particular the four neutron absorbing scintillators, will affect the neutron flux distribution. The consequences of such a flux distortion are usually not significant when measuring the scalar flux. However, the gradient is estimated from the difference of two values of the neutron flux, measured relatively close to each other, and hence it is obtained as the small difference of two values close to each other. If the distorting effect of the four scintillators is not uniform, then the presence of the detector may have a much more substantial effect on the accuracy of the determination of the flux gradient than for the scalar flux. Second, systematic distortions might arise from a self-shielding effect, i.e., the scintillators at the higher flux position might shield against the neutron current pointing to the scintillators at the lower flux position. If the effect is relevant, then the detector will systematically underestimate the gradient. Such a possible consequence needs to be investigated quantitatively.

The simulations performed in this work are restricted to the neutronic aspects of the measurement, i.e. calculating the reaction rates in the detector. That is, the generation and transport of the scintillation light is not taken into consideration. The reason for this is that the effects to be studied, such as the influence of the presence of the detector on the estimation of the gradient, is a pure neutronic problem. Although the conversion of the neutron reactions inside the detector into scintillation light, photon transfer to and transport in the fiber, etc. are an important part of the physics of the measurement, which influence the efficiency of the detector, these processes are not relevant from the point of view of the objectives of the present study. Including the light generation and transport into the simulations would require a substantially larger effort, with minimal extra information.

The quantitative work for the assessment of the performance of the detector was made using the open-source code Serpent [13]. Serpent is a multi-purpose three-dimensional continuous-energy Monte Carlo

particle transport code developed at VTT, the Technical Research Centre of Finland. The code is designed for traditional reactor physics applications, for multi-physics reactor calculations, and for neutron and photon transport calculations in radiation, fusion and medical physics problems. Serpent also includes numerical capabilities that allow parallel computing on clusters and multi-core workstations.

The strategy to quantify the perturbative effect of the presence of the detector on the accuracy of the determination of the flux gradient goes as follows. Given a system of interest, two sets of simulations are performed. The first simulation does not include the detector and the “unperturbed” thermal neutron flux is calculated in some hypothetical measurement positions where the gradient detector can be inserted. In the second step, simulations are made for the case that the detector is occupying the positions previously selected, one at a time, and the reaction rates in the scintillators are calculated. The gradient obtained from the difference of the reaction rates of the diagonally opposite scintillator pairs is then compared with the gradient of the neutron flux obtained without the detector.

The comparison of the gradient from the unperturbed flux with the gradient from the reaction rates is, however, not completely trivial. It is obvious from simple physical considerations that at any single measurement point, the magnitude of the gradient will be quantitatively different for the flux and the reaction rate, since they correspond to physically different quantities. Nevertheless, the two are proportional to a scaling factor which can be considered as a constant when the energy distribution of the flux in the system is also constant (this is indicated in Fig. 5, showing that the thermal spectrum even inside the source itself is very similar to that in water). The scaling factor does not depend on the actual value of the gradient, and hence on the measurement position. Then the proof of the equivalence is based on the equivalence of the space dependence of the two gradients. If the space dependence of the two gradients is proportional to a constant scaling factor, then it is a demonstration of the negligible effect of the presence of the detector on the measurement of the flux gradient.

The existence of a proportionality factor between the flux gradient and the gradient of the detector response is by no means a problem for the task of localizing an unknown perturbation, or an unknown source. Such a task is always based on relative values (ratios of the flux, or its gradient, as measured in different space points) because in a practical case the strength of the source is not known. Therefore the absolute values of the flux or the gradient are not of interest anyway. The diagnostic information lies in the space dependence of the gradient, and it is this latter which should be reconstructed correctly.

As mentioned above, the first step with Serpent was to calculate the spatial distribution of the neutron flux in a hypothetical arrangement without the presence of the detector, in which thereafter measurements with the proposed detector would be simulated. The arrangement was chosen to be similar to those used in earlier works, namely the case of a neutron source in a water tank [5,6]. The reason is partly that it is a simple setup, with an azimuthally symmetric flux distribution in the horizontal plane, in which the results can be easily interpreted intuitively. And partly, because such an experiment will be possible to carry out at a later stage of the project, when the detector will actually be fabricated. The general layout is shown in Fig. 3. It consists of a cylindrical Aluminum tank 1 m in height and 1 m in diameter filled with water, with a  $^{252}\text{Cf}$  source, 2 cm in diameter, in the middle.

The next step was the modeling of the part of the gradient detector which are called “scintillators” in this paper. There exist several different options for small size neutron detectors in terms of neutron converter and scintillation material (LiCaF, boron loaded plastic scintillator, etc.). We restrict the present study to the type of detectors which we have at hands and which were also used in previous works, namely LiF as neutron converter and ZnS(Ag) as the scintillation material. Two such detectors are available by courtesy of Kyoto University Institute for Integrated Radiation and Nuclear Science (KURNS). The detailed Serpent model of the detector is shown in Fig. 4.

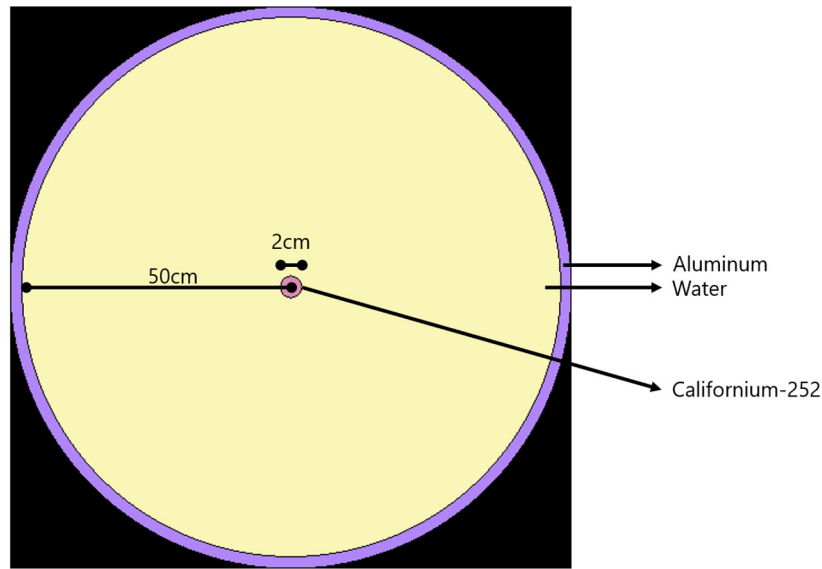


Fig. 3. Setup used for the evaluation of the detector, as modeled in Serpent.

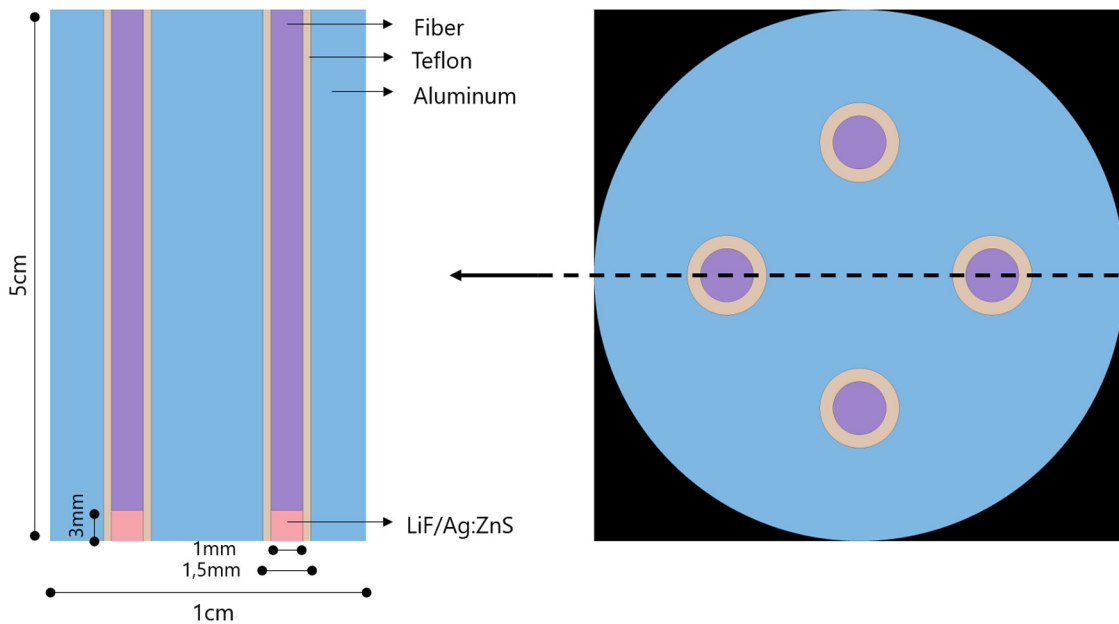


Fig. 4. The LiF-based gradient detector as modeled in Serpent.

#### 4. Quantitative analysis

The Serpent model of the test case is used to analyze the energy and space dependence of the neutron flux due to the  $^{252}\text{Cf}$  source in the water tank. Then simulations were performed to study the performance of the proposed detector to estimate the neutron flux gradient in such a test case.

##### 4.1. Estimation of the neutron flux in the test case

Sample results of the energy and space dependence of the neutron flux estimated for the source in the water tank are shown in Figs. 5 and 6, respectively. Far away from the source (indicated as “Water” in the figure), a thermalized spectrum is seen. Inside the sample ( $^{252}\text{Cf}$  in the figure legend), in the thermal region the spectrum is very similar

to that in the water, in the epithermal region one can see the fission resonances inside the sample, and the fast spectrum is determined by the spectrum of the spontaneous fission of the  $^{252}\text{Cf}$  source.

Regarding the space dependence, the thermal flux is of primary interest, since the detector is assumed to be sensitive to thermal neutrons. The space dependence of the thermal flux shown in Fig. 6 is similar to the one found in the previous experiments, although a different type of source was used. The thermal flux decays with increasing distance from the source, but this decrease is not monotonic. There is a dip in the vicinity of the source, which is due to the absorption of the thermal neutrons in the source itself. This space dependence is suitable for the investigation of the performance of the detector, because there are positions with both small and high flux gradients, the radial component changing from positive to negative with increasing distance from the center. In order to verify the Serpent model, the calculations were also

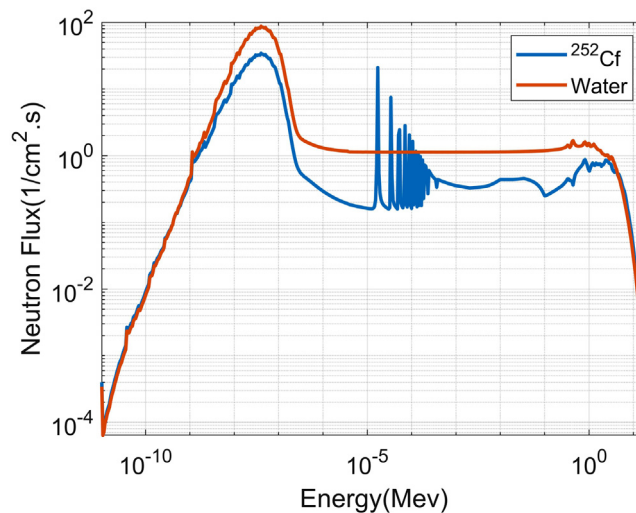


Fig. 5. The energy spectrum of the neutrons in the  $^{252}\text{Cf}$  source and in the surrounding water.

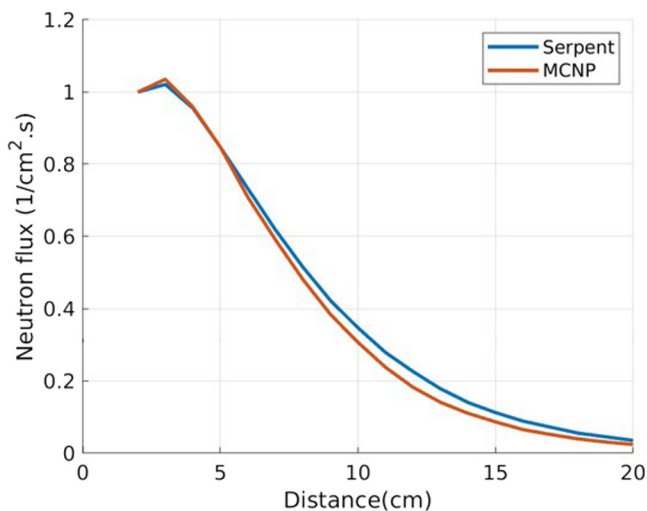


Fig. 6. The radial dependence of thermal neutrons in the measurement setup.

performed with the Monte Carlo code MCNP [14]. Fig. 6 shows that the results from the two codes are in good agreement.

#### 4.2. Investigation of the performance of the detector

The performance of the detector to determine the magnitude and the direction of the neutron flux gradient was investigated via Monte Carlo calculations in the case of the setup defined in Section 3. Different positions and orientations of the detector in the water tank, and the effect of scintillators with non-ideal  $^6\text{Li}$  content were considered.

##### 4.2.1. Estimation of the magnitude of the gradient

As mentioned in Section 3, one goal is to investigate how the presence of the detector affects the accuracy of the estimation of the gradient. In this step, we chose a detector orientation such that two scintillators were lined up on the  $x$ -axis, i.e. the line connecting two of the scintillators was pointing to the source (towards the center of the water tank). Because of the azimuthal symmetry of the setup, these two scintillators measure the radial gradient (i.e. its  $x$ -component), and the azimuthal component of the flux gradient is zero. Hence, the radial component is equal to the absolute value (magnitude) of the gradient. The Serpent model of this arrangement is shown in Fig. 7.

Calculations were made by including the detector in the setup. The reaction rates in the four scintillators of the detector were calculated. To assess the possible distorting effect of the detector, as described in Section 3, the gradient was calculated both from the neutron flux which prevails in the system without the detector, as well as from the reaction rate in the scintillators, with the whole detector being included into the simulations.

The comparison of the space dependence of the flux gradient and the gradient based on the reaction rate is shown in Fig. 8. The space dependence of the gradient, determined from the reaction rates in the detector, follows very closely the space dependence of the gradient of the unperturbed flux over the whole spatial measurement range, indicating that the distortion effect of the proposed detector design is negligible.

##### 4.2.2. Estimation of the direction of the gradient vector

The two-dimensional flux gradient has two Cartesian components which carry independent information. For practical purposes, instead of using these two components, the space dependence of the magnitude (absolute value) of the gradient and its direction are used in unfolding problems. This is because the absolute value and the direction are concepts with a physical content that is easier to interpret intuitively. One can see an analogy with the case of complex valued physical quantities, such as Fourier transforms of time dependent signals in the frequency domain, where the amplitude and phase have clear physical meaning, as opposed to that of the real and imaginary parts individually. From the point of the planned application, the magnitude and direction are more effective feature parameters in a pattern recognition or any other identification/unfolding task than the vector Cartesian components.

Therefore, it is useful to investigate the suitability of the detector to estimate the direction of the gradient vector. The best way of doing this is when both components of the gradient are different from zero. In the present setup, this means that the detector needs to be positioned such that none of the two scintillator pairs lie on a radial line (i.e. along the  $x$  axis in a Cartesian system). Other special orientations are also avoided, e.g., when the angle between the two scintillator lines and the  $x$  axis is  $\pm 45^\circ$ . Then, we chose a setup where the detector was rotated  $30^\circ$  counterclockwise as compared to the calculations in the previous Subsection. An illustration of this case is shown in Fig. 9.

The detector measures the two components of the gradient in the coordinate system determined by its own orientation, but the orientation of the measured gradient vector is naturally independent from the orientation of the detector as shown in Fig. 10. We performed several simulations with assuming the detector at different positions along the  $x$  axis, and the results of the direction of the gradient vector from the

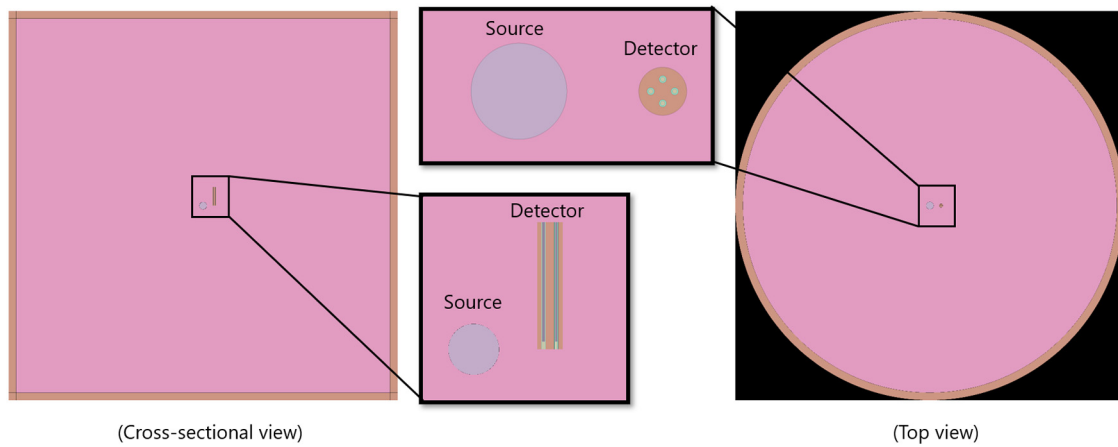


Fig. 7. The Serpent model for the simulation of the measurement of the radial component of the gradient.

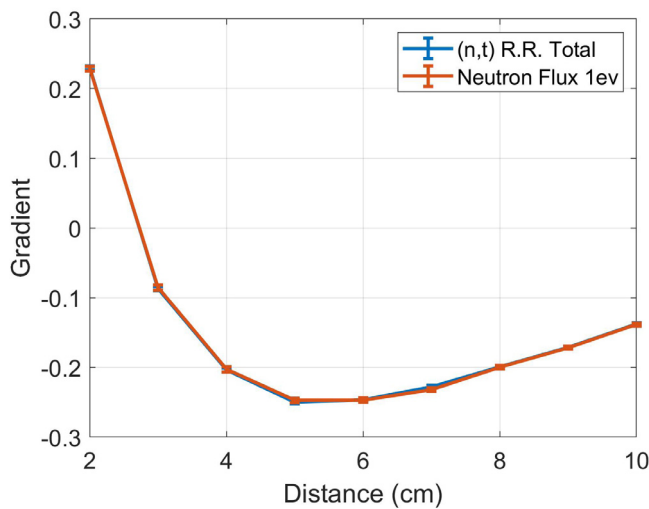


Fig. 8. The spatial dependence of the radial component of the gradient with and without the presence of the detector.

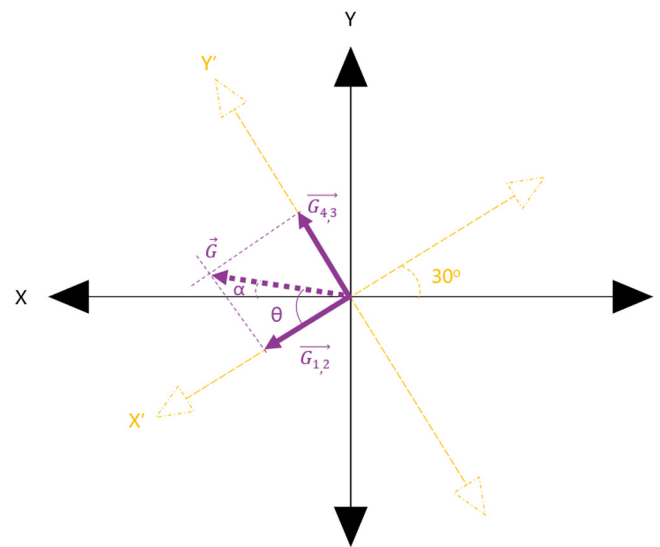


Fig. 10. The detector coordinate system based on its orientation (yellow) the original coordinate system of the measurement setup (black) and the two components of the gradient vector (purple). (For interpretation of the references to color in this figure legend, the reader is referred to the web version of this article.)

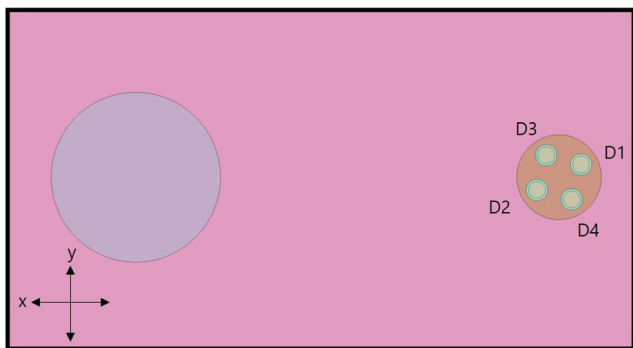


Fig. 9. The Serpent model of the measurement of the direction of the gradient showing the detector shifted in a 30° angle counterclockwise.

calculated reaction rates are shown in Fig. 11. The direction angle of the gradient is estimated correctly.

To prove the consistency of the performance of the detector, the magnitude (as an absolute value) of the gradient vector measured by the detector was compared between the case where the gradient was calculated from only the horizontal component as in Section 4.2.1 (normal case) and the case where the gradient was calculated from

Table 1

A comparison of the magnitude of the gradient vector.

Distance (cm)	Magnitude of the gradient			
	Normal case		30° angle shift	
	Value ( $\times 10^{-3}$ )	Uncertainty (%)	Value ( $\times 10^{-3}$ )	Uncertainty (%)
2	3.77	1.22	3.86	2.04
5	-4.10	1.05	-4.01	1.61
10	-2.26	1.07	-2.28	1.58

the two components after it was shifted by a 30° angle. The values of the magnitude of the gradient in the two cases, at different positions along the x-axis, are listed in Table 1. It can be seen that the detector is capable of giving similar values of the magnitude of the gradient regardless of its orientation.

#### 4.2.3. Effect of the differences in the scintillators of the detector

In the simulations so far, it was assumed that all four scintillators are equal and thus have the same efficiency. In a real detector, the four scintillators may slightly differ from each other, especially in view of their manual manufacturing procedure. This incurs that the amount of neutron converter and scintillation material is not strictly controlled,

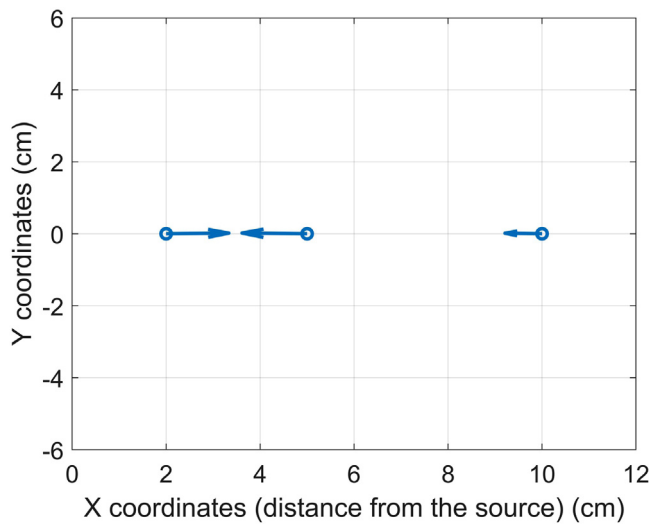


Fig. 11. The direction of the gradient vector at different placements of the detector along the  $x$ -axis.

and is likely to have different values in the individual scintillators. This problem can of course be minimized in various ways. One possibility is to use the emerging technology of 3D printing, by which the volume of the sensitive part of the scintillator can be controlled with high precision. Further, the scintillators can also be calibrated in laboratory measurements, and to use the calibration factors to correct the measured values.

However, a quantitative investigation of the effect of the different sensitivities of the scintillators, and the methods for correcting them, are still of interest. Even if the efficiency of the individual scintillators can be calibrated in laboratory measurements separately, these efficiencies may not be the same for the scintillators after they are mounted in the detector. The mounting material, the surrounding matrix, the optical coupling of the fiber to both the scintillator and the PM tube will affect the individual performances. This means that after the scintillators are mounted in the detector, their individual efficiencies become more complicated to determine.

On the other hand, one does not need to determine the absolute efficiencies of the four scintillators, only the efficiencies relative to each other, and elaborate methods to compensate for them. As mentioned earlier, the flux gradient is only determined to a constant scaling factor, whose value is not of interest. With scintillators of different sensitivities, this scaling factor would not be constant, but would depend, e.g., on the detector orientation. The purpose of the correction is thus to make sure that a constant scaling is preserved, irrespective of the orientation of the detector. Such correction methods will be quantitatively investigated in the forthcoming. The correction method used in the current study as discussed below amounts to an in-situ calibration of the relative efficiencies, which can be even performed in a field measurement, and has to be executed only once.

In order to investigate the effect of having imperfect scintillators on the estimation of the flux gradient, 4 scenarios were considered. In the first scenario, one of the four scintillators is altered to have a lower atomic fraction of  ${}^6\text{Li}$  and hence a lower efficiency. The second case is such that the detector defined in the first scenario is tested with a different orientation. In the third scenario, the gradient detector consists of 4 scintillators with a different content of  ${}^6\text{Li}$ . In the fourth scenario, the detector with 4 different scintillators is studied adding a possible uncertainty to the initial position and the rotation angles.

#### Detector with one scintillator with different ${}^6\text{Li}$ content

In the first simulation, we chose an arrangement in which the two diagonally opposite scintillators D1 and D2 (see Fig. 9 for the notations)

Table 2

The effect of having one of the four scintillators at a lower efficiency on the estimation of the flux gradient.

Case	Position (Distance from the source)			
	3 cm		6 cm	
	Value ( $\times 10^{-3}$ )	Uncertainty (%)	Value ( $\times 10^{-3}$ )	Uncertainty (%)
Ideal case <sup>a</sup>	-1.43	3.45	-4.05	0.97
Non-ideal case <sup>b</sup>	-1.37	2.50	-3.91	0.71
Ratio <sup>c</sup>	958	1.21	965	4.23

<sup>a</sup>The ideal case of having the four scintillators at 100% efficiency.

<sup>b</sup>The case where D1 is at a lower efficiency (the atomic fraction of  ${}^6\text{Li}$  was reduced to 80% of its original value).

<sup>c</sup>The ratio between the gradient estimated from the non-ideal case to the one estimated from the ideal case.

were lined up on a radial line, hence measuring the radial component of the gradient. Since the azimuthal component of the gradient is zero, we only need to consider these two scintillators (similarly to the case presented in Section 4.2.1). Two positions of the gradient detector were chosen; one at 3 cm from the source, and another at 6 cm. In the first, the magnitude of the gradient is very low (as seen from the previous results) and is expected to reflect the maximum biasing effect of having different scintillator efficiencies. The other point lies at a position of high flux gradient, 6 cm from the source. The material composition of only one of the four scintillators (D1) was altered to have a lower efficiency than the other three. In the sensitive part of scintillator D1 the atomic fraction of  ${}^6\text{Li}$  was reduced to 80% of its original value.

One single measurement in a point would give a biased value of the gradient, due to the different sensitivities of D1 and D2. One obvious way to compensate for the difference between D1 and D2 is to perform two measurements at the same location, the first one with the detector in its original orientation, and the second one by rotating the detector by  $180^\circ$ , such that D1 and D2 swap their positions. By taking the average between the respective values of the gradients obtained from the two measurements leads to an unbiased estimation of the gradient.

The results of such a simulation are listed in Table 2. The calculated magnitude of the gradient is slightly underestimated compared to the ideal case (i.e., when both D1 and D2 have 100% efficiency). The underestimation of the magnitude of the gradient is expected, and is simply due to the lower total efficiency of the detector.

Similar to the measurements with perfectly identical scintillators, the absolute value of the gradient does not bear any significance. Again, the important fact is that the space dependence of the gradient obtained from this procedure is the same as that of the true gradient of the thermal flux. One way of investigating this in the present case is to see whether the ratio between the gradients obtained by D1 and D2 with equal and different sensitivities respectively, is constant, regardless of the position of the detector. The last row of Table 2 shows that the ratio between the two quantities indeed is very close to each other in the two different spatial positions, indicating that the method of compensating for the different scintillator efficiencies is applicable. For this procedure, the actual difference in the sensitivities does not need to be known.

#### Detector with one scintillator with different ${}^6\text{Li}$ content and different orientation

One potential weakness of the above mentioned correction method is that, when the detector is inserted several meters into the guide tube of a fuel assembly, its orientation may not be possible to control (or to know) with 100% precision. This is valid for both the uncertainty of the original positioning, as well as the inaccuracy of the magnitude of the rotation. In order to quantify the effect of the uncertainty in the detector orientation, the same simulation was repeated with a rotation of the detector according to  $175^\circ$  instead of a perfect  $180^\circ$ . This slight difference in the rotation angle has a correspondingly little effect on the estimation of the gradient, as is seen in Table 3.



**Table 3**

The effect of added uncertainty in the rotation angle on the estimation of the flux gradient.

Case	Position	
	3 cm	
	Value ( $\times 10^{-3}$ )	Uncertainty (%)
Ideal case	-1.43	3.45
Non-ideal case	-1.37	2.50
Non-ideal case (175°) <sup>a</sup>	-1.37	2.48

<sup>a</sup>The case where D1 is at a lower efficiency and the rotation angle was set to 175° instead of 180°.

### Detector with scintillators with different <sup>6</sup>Li content

A further step is a more general scenario in which both the measured components of the gradient are non-zero, and all four scintillators have different sensitivities. This latter was achieved in the simulations by leaving one of the efficiencies unchanged, and changing the efficiencies of the other three scintillators to various degrees. The atomic fraction of <sup>6</sup>Li was reduced for D2, D3 and D4 to 80%, 70% and 60% respectively, and kept at 100% for D1. The detector was again placed at 3 cm from the source but this time rotated by a 30° angle counterclockwise as the starting orientation. This experimental arrangement will result in both measured components of the gradient being non-zero.

Based on the foregoing, one might think that, to obtain an unbiased estimate of the two components of the gradient vector, it is sufficient to rotate the detector with 180°, such that D1 and D2, as well as D3 and D4, respectively, swap positions. Although with such a procedure one indeed gets a scaling of both components of the gradient which is independent of the measurement position, it is also easy to see that with this method, in general, the direction of the gradient would be determined incorrectly, i.e. it would contain a bias. This is because the scaling is linearly proportional with the total efficiency of D1 + D2 for one component, and with the total efficiency of D3 + D4 for the other. If these two total efficiencies are not equal to each other, then the two components will be scaled differently, leading to a bias in the determination of the direction of the gradient vector.

For an unbiased estimate of the direction of the gradient vector, the detector needs to be rotated three times with 90° at a time, i.e. rotating the detector by 90°, 180° and 270° from its original orientation. Then each scintillator occupies each of the four angular positions once. The average value of the four reaction rates at each measurement position is then calculated, and the two components of the gradient are determined by taking the difference of the average reaction rates in the diagonally opposing positions.

The results of such a simulation are shown in Table 4 and Fig. 12. The estimated magnitude of the gradient with the four scintillators characterized by different fractions of <sup>6</sup>Li is smaller than in the case of four identical scintillators (see Table 4), which is a direct consequence of the fact that the efficiencies of 3 scintillators are reduced. On the other hand, despite of the different efficiencies of the scintillators, the detector is capable of providing the expected direction of the gradient vector (see Fig. 12). Again, this procedure does not require knowledge of the individual sensitivities.

Naturally, a measurement procedure which requires four sub-measurements in one spatial position to obtain the two components of the gradient is not useful in practice. If each scintillator needs to be placed in each of the four angular positions, then in principle it would suffice to use only one scintillator, and put it sequentially in the four designated positions. In that case the problem with the different efficiencies would not occur, and there would be no need for an averaging procedure either.

However, the measurement of the gradient vector with one gradient detector without the need of rotating it is the method to be preferred.

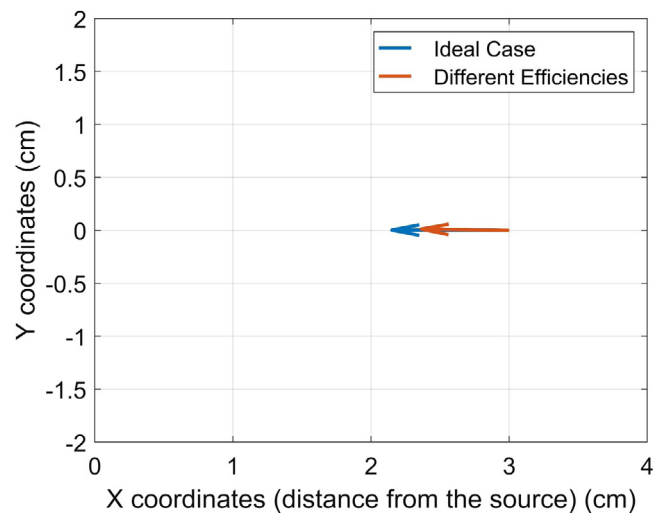


**Fig. 12.** The effect of the different scintillator efficiencies on the estimation of the direction of the gradient vector. (For interpretation of the references to color in this figure legend, the reader is referred to the web version of this article.)

**Table 4**

The effect of different scintillator efficiencies on the estimation of the magnitude of the flux gradient.

Case	Position	
	3 cm	
	Value ( $\times 10^{-3}$ )	Uncertainty (%)
Ideal case <sup>a</sup>	-1.46	3.12
Non-ideal case <sup>b</sup>	-1.22	2.61

<sup>a</sup>The ideal case of having the four scintillators at 100% efficiency with the detector rotated by a 30° angle as the starting orientation.

<sup>b</sup>The case where D2, D3 and D4 is at a varying lower efficiencies than D1.

**Table 5**

The estimation of the relative efficiencies of the four scintillators.

Relative efficiency	Scintillators			
	D <sub>1</sub>	D <sub>2</sub>	D <sub>3</sub>	D <sub>4</sub>
D <sub>i</sub> /D <sub>1</sub> , i = 1, ..., 4	100%	92.1%	87%	81.2%

Apart from the option of manufacturing scintillators with equal efficiencies, another possibility is to make four separate measurements by rotating the detector three times, amounting to an in-situ relative calibration of the individual scintillator efficiencies. This is achieved such that the reaction rates of each scintillator in the four angular positions are added up individually. If all scintillators had the same efficiency, then these four total reaction rates would be equal. If the efficiencies are different, this will be reflected in the total reaction rates of the scintillators, taken in the four orientations. The total reaction rates are linearly proportional to the individual efficiencies. One such measurement with the original position plus three rotations of the detector can be used to determine the relative efficiencies, which can be used to correct the measurements in other points, without the need of rotating the detector.

The feasibility of this method was investigated using the previous simulation, in which the detector is placed at 3 cm from the source and the <sup>6</sup>Li content in the four scintillators is known (i.e., 100%, 80%, 70% and 60% of the nominal value for D1, D2, D3 and D4, respectively). The individual relative efficiencies of the detectors were estimated from the count rate ratios D<sub>i</sub>/D<sub>1</sub>, i = 1...4, see Table 5. These results show that the relation between <sup>6</sup>Li contents and relative performances of the scintillators is not linear. For example, the scintillator D4 has an

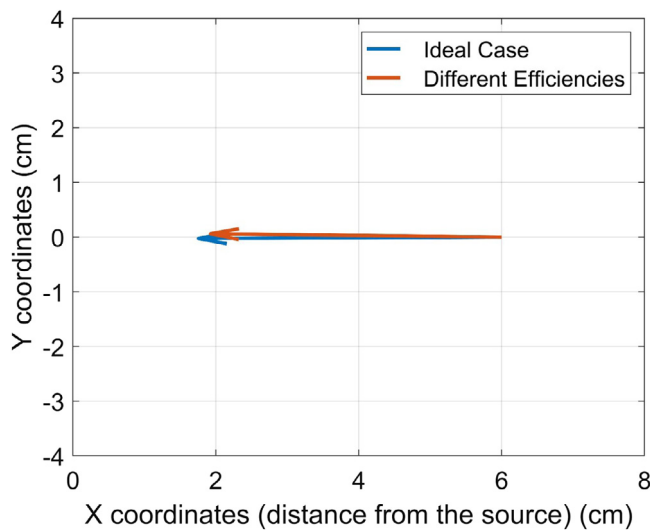


Fig. 13. The estimation of the direction of the gradient vector from the calibrated detector at 6 cm from the source. (For interpretation of the references to color in this figure legend, the reader is referred to the web version of this article.)

efficiency of 81.2% with respect to D1, although its  ${}^6\text{Li}$  fraction is only 60%.

Another measurement was simulated with the detector positioned at 6 cm from the source. This simulation was also made with the detector being rotated  $30^\circ$  counterclockwise as its initial position. The calculated reaction rates were then divided by the individual relative efficiencies derived from the previous step (see Table 5).

The resulting direction of the gradient vector is unfolded correctly with the calibration procedure, as shown in Fig. 13.

#### Detector with scintillators with different ${}^6\text{Li}$ content and different rotations

The possible source of error of incorrect orientation of the detector was further investigated by comparing the direction of the gradient vector from the ideal case with two other cases as shown in Fig. 14. The ideal case (represented by the blue arrow in Fig. 14) is when the four scintillators have the exact same material composition and the detector is placed accurately at  $30^\circ$  as its initial orientation. The second case (red arrow) is when the four scintillators have the same material composition but an error was introduced to the initial orientation angle, i.e., the detector is shifted of  $27^\circ$  with respect to the  $x$ -axis. The third case (yellow arrow) is when the four scintillators have different atomic fractions of  ${}^6\text{Li}$  (100%, 80%, 70%, 60% for D1, D2, D3 and D4 respectively) and an error was introduced to the rotation angles during the calibration. In this particular case the detector was rotated with  $92^\circ$ ,  $179^\circ$  and  $273^\circ$ , instead of  $90^\circ$ ,  $180^\circ$  and  $270^\circ$ , respectively.

The results show that an accurate reconstruction of the direction of the gradient vector is still possible despite the possible random uncertainty in the initial positioning or the rotation angles of the detector. It can also be noticed that the estimation of the direction was even more accurate in the case where the detector needed to be rotated four times than the case where the only source of error was in the initial positioning of the detector, which is probably due to the fact that random errors that arise from the four rotations tend to compensate for each other, which leads to a lower total error in the end.

The results of the reaction rates from the case described above, where the four scintillators had different material compositions and an uncertainty was introduced to the four rotation angles, were again used to estimate the relative efficiencies of the four scintillators. The results show that the presence of the uncertainty in the rotation angles had a very small effect on the estimation of the relative efficiencies of the four scintillators and the results were identical to the ones presented in

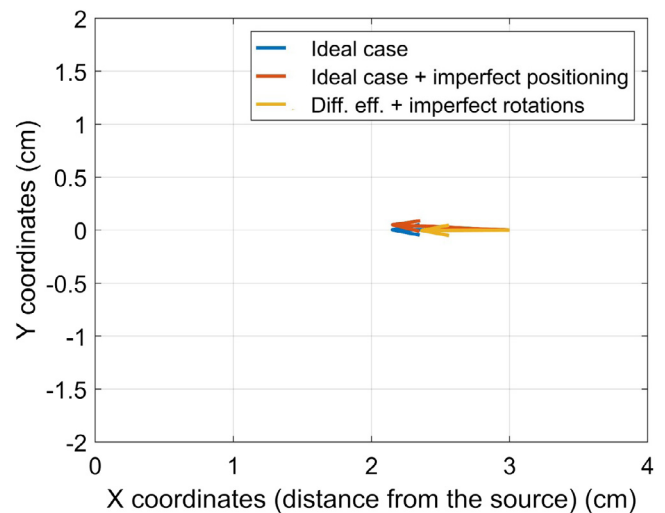


Fig. 14. The effect of random uncertainties in the initial positioning and the rotation angles on the estimation of the direction of the flux gradient. (For interpretation of the references to color in this figure legend, the reader is referred to the web version of this article.)

Table 5. Hence, the method is still applicable for the calibration process and the correction the gradient along with its direction at other spatial positions.

## 5. Conclusion

In this paper the design of a new neutron detector, capable of measuring the gradient of the neutron flux within a fuel assembly has been suggested and evaluated using Monte Carlo simulations. The detector allows measuring the magnitude and direction of the neutron gradient vector within a multiplying or scattering neutron system. The detector is based on four thin LiF/ZnS(Ag) optical fiber-mounted neutron scintillators arranged in an aluminum matrix according to a rectangular pattern. The detector can be used to estimate the two components of the gradient of the scalar neutron flux, from the difference between the measurements provided by the diagonally-opposite pairs of scintillators.

The detector was modeled and its performances simulated in a hypothetical setup with a  ${}^{252}\text{Cf}$  neutron source in a water tank. It was shown that the determination of the gradient vector is feasible, i.e. the presence of the detector and associated shielding effects do not introduce significant distortion of the flux which would make the determination of the gradient inaccurate. It was also found that differences from the ideal composition of the scintillators and from their orientations with respect to the neutron source have a minor influence on the calculated gradient.

Future work is planned to study the detector in a full fuel assembly (instead of the simple case of a neutron source in a water tank) and its performance to identify possible local inhomogeneities (e.g., a missing fuel pin in the assembly). Manufacturing and testing of the proposed detector has already started.

## Declaration of competing interest

The authors declare that they have no known competing financial interests or personal relationships that could have appeared to influence the work reported in this paper.

## Acknowledgments

The computations presented in this paper were enabled by resources provided by the Swedish National Infrastructure for Computing (SNIC) at the Chalmers Centre for Computational Science and Engineering (C3SE), and at the National Supercomputer Centre (NSC), Linköping University (LiU), partially funded by the Swedish Research Council through grant agreement no. 2018-05973. The project was also financially supported by the Swedish Radiation Safety Authority, and the Ringhals power plant, Sweden. We are grateful for Profs. T. Misawa, Y. Kitamura and Dr. Y. Takahashi, Institute for Integrated Radiation and Nuclear Science, Kyoto University (KURNS), for providing us two fiber neutron detectors.

## References

- [1] I. Pázsit, O. Glöckler, On the neutron noise diagnostics of pressurized water reactor control rod vibrations III. Application at a power plant, *Nucl. Sci. Eng.* 99 (4) (1988) 313–328.
- [2] J.K.-H. Karlsson, I. Pázsit, Localisation of a channel instability in the Forsmark-1 boiling water reactor, *Ann. Nucl. Energy* 26 (13) (1999) 1183–1204.
- [3] I. Pázsit, On the possible use of the neutron current in core monitoring and noise diagnostics, *Ann. Nucl. Energy* 24 (15) (1997) 1257–1270.
- [4] V. Arzhanov, I. Pázsit, N.S. Garis, Localization of a vibrating control rod pin in pressurized water reactors using the neutron flux and current noise, *Nucl. Technol.* 131 (2) (2000) 239–251.
- [5] P. Lindén, J.K.-H. Karlsson, B. Dahl, I. Pázsit, G. Por, Localisation of a neutron source using measurements and calculation of the neutron flux and its gradient, *Nucl. Instrum. Methods A* 438 (2–3) (1999) 345–355.
- [6] S. Avdic, P. Lindén, I. Pázsit, Measurement of the neutron current and its use for the localisation of a neutron source, *Nucl. Instrum. Methods A* 457 (3) (2001) 607–616.
- [7] S. Avdic, P. Lindén, B. Dahl, I. Pázsit, Determination of the neutron current and diagnostic application in an experimental system., *Nucl. Tehnol.* 2 (2001) 34–40.
- [8] C. Mori, T. Osada, K. Yanagida, T. Aoyama, A. Uritani, H. Miyahara, Y. Yamane, K. Kobayashi, C. Ichihara, S. Shiroya, Simple and quick measurement of neutron flux distribution by using an optical fiber with scintillator, *J. Nucl. Sci. Technol.* 31 (3) (1994) 248–249.
- [9] T. Yagi, H. Unesaki, T. Misawa, C.H. Pyeon, S. Shiroya, T. Matsumoto, H. Harano, Development of a small scintillation detector with an optical fiber for fast neutrons, *Appl. Radiat. Isot.* 69 (2) (2011) 539–544.
- [10] R. Rossa, A. Borella, N. Giani, Comparison of machine learning models for the detection of partial defects in spent nuclear fuel, *Ann. Nucl. Energy* 147 (2020) 107680.
- [11] H. Lee, M.-S. Yim, Investigation of a fast partial defect detection method for safeguarding PWR spent fuel assemblies, *Ann. Nucl. Energy* 144 (2020) 107496.
- [12] R. Rossa, A. Borella, K. van der Meer, Comparison of the SINRD and PDET detectors for the detection of fuel pins diversion in PWR fuel assemblies, in: *Proc. INMM-59 Annual Meeting*, 2018.
- [13] J. Leppänen, The Serpent Monte Carlo code: Status, development and applications in 2013, *Ann. Nucl. Energy* 82 (2015) 142–150.
- [14] C.J. Werner, MCNP6.2 Release Notes, Los Alamos National Laboratory, 2018.